

# The Innermost Stable Circular Orbit in Compact Binaries

Thomas W. Baumgarte

*Department of Physics, University of Illinois at Urbana-Champaign, Urbana, IL 61801*

**Abstract.** Newtonian point mass binaries can be brought into arbitrarily close circular orbits. Neutron stars and black holes, however, are extended, relativistic objects. Both finite size and relativistic effects make very close orbits unstable, so that there exists an innermost stable circular orbit (ISCO). We illustrate the physics of the ISCO in a simple model problem, and review different techniques which have been employed to locate the ISCO in black hole and neutron star binaries. We discuss different assumptions and approximations, and speculate on how differences in the results may be explained and resolved.

## INTRODUCTION

Compact binaries, containing black holes or neutron stars, are among the most promising sources for the new generation of gravitational wave detectors. TAMA has already started taking data, and LIGO, VIRGO and GEO will soon become operational (see, e.g., [1]). With the advent of gravitational wave astronomy arises a need for theoretical templates of gravitational waveforms, which are required for the identification and interpretation of signals in the noisy output of the detectors.

Compact binaries emit gravitational radiation, and therefore lose energy and slowly spiral towards each other. Because of the circularizing effects of gravitational radiation damping, it is reasonable to assume the orbits of close binaries to be quasi-circular. The slow and adiabatic inspiral continues until the binary reaches the innermost stable circular orbit (ISCO), at which the orbits become unstable. At that point, the stars start to plunge towards each other, and coalesce and merge after a dynamical timescale. The ISCO leaves a characteristic signature in the gravitational wave signal of a binary inspiral, and therefore provides an important piece of information for the construction of gravitational wave templates.

In this article, we will explain in a simple point-mass model problem how both tidal and relativistic effects make very close orbits unstable, giving rise to the ISCO. We will then review attempts to determine the ISCO for binary black holes, which, for stellar-mass black holes, is likely to fall into the frequency range of LIGO. In particular, we will compare results from post-Newtonian (PN) and numerical calcu-

lations. We will also discuss some of the qualitative results for binary neutron stars, and will summarize some of the more recent results from relativistic simulations.

## THE ISCO IN A SIMPLE MODEL PROBLEM

Most commonly, the ISCO is located with the help of turning-point methods. We motivate this method by applying it to Newtonian point-masses, and introduce tidal and relativistic correction terms to illustrate their effect. Rigorous justifications for turning-point methods have been developed, for example, in [2–4].

### Newtonian point-masses

The conditions for a circular orbit can be derived very easily from the Hamiltonian formalism. Consider, for example, a Newtonian point mass binary, for which the energy is the sum of the kinetic and potential energy

$$E = \frac{1}{2}\mu \dot{\mathbf{r}}^2 - \frac{\mu M}{r} = \frac{1}{2}\mu(\dot{r}^2 + r^2\Omega^2) - \frac{\mu M}{r}. \quad (1)$$

Here  $M \equiv m_1 + m_2$  is the total mass,  $\mu \equiv m_1 m_2 / M$  the reduced mass,  $\mathbf{r}$  the separation vector, and  $\Omega = \dot{\varphi}$  the angular velocity. Rewriting the energy in terms of the conjugate momenta  $P = \mu \dot{r}$  and  $J = \mu r^2 \Omega$  yields the Hamiltonian

$$E = H = \frac{1}{2} \frac{P^2}{\mu} + \frac{1}{2} \frac{J^2}{\mu r^2} - \frac{\mu M}{r}. \quad (2)$$

The four independent variables  $r$ ,  $P$ ,  $\varphi$  and  $J$  now satisfy the Hamiltonian equations

$$\begin{aligned} \dot{r} &= \frac{\partial H}{\partial P} & \dot{P} &= -\frac{\partial H}{\partial r} \\ \Omega = \dot{\varphi} &= \frac{\partial H}{\partial J} & \dot{J} &= -\frac{\partial H}{\partial \varphi} = 0. \end{aligned} \quad (3)$$

The last equation shows that the angular momentum is conserved, since the Hamiltonian is cyclic in  $\varphi$ . To construct a circular orbit, we obviously need  $\dot{r} = 0$ , which implies  $P = 0$ , and also  $\dot{P} = 0$ , so that

$$\left. \frac{\partial H}{\partial r} \right|_J = \left. \frac{\partial E}{\partial r} \right|_J = 0. \quad (4)$$

A circular orbit hence corresponds to an extremum of the energy at constant angular momentum. The orbital frequency of a circular orbit can be determined from

$$\Omega = \frac{\partial H}{\partial J} = \frac{\partial E}{\partial J}. \quad (5)$$

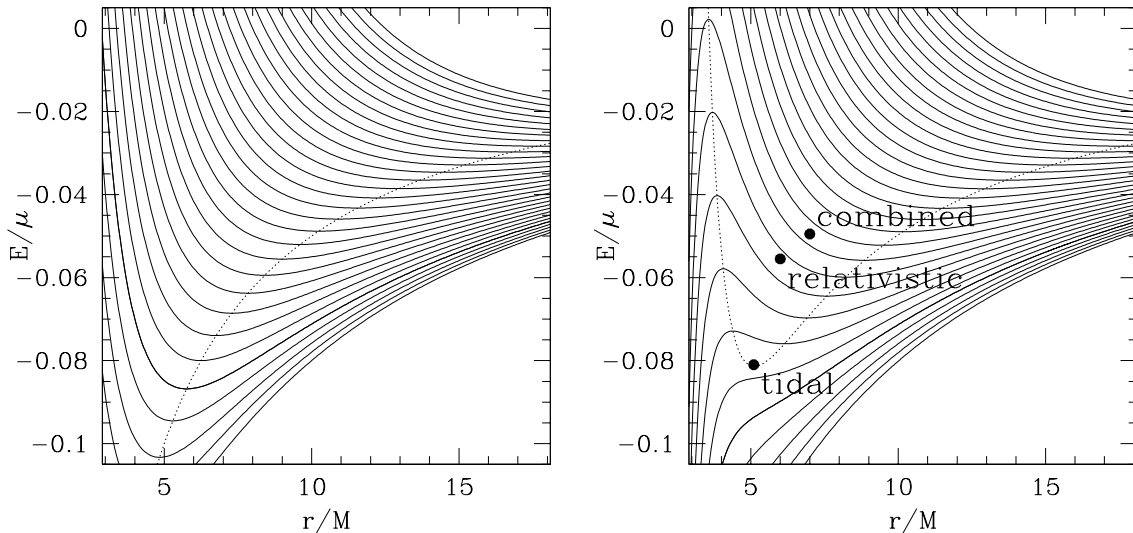


**FIGURE 1.** Energy as function of separation for a Newtonian point mass binary (left panel), and a model problem including tidal effects (right panel, see text). The solid lines are contours of constant angular momentum  $J$ , with the values of  $J$  increasing from the bottom to the top. The extrema of these contours correspond to circular orbits (eq. (4)). The dashed line connects the circular orbits and represents the equilibrium energy  $E_{\text{eq}}$ , and the dots mark the ISCO for tidal, relativistic and combined effects.

The last two equations are crucial for the construction of the ISCO.

Returning to the example of a Newtonian point mass binary, we can construct circular orbits by inserting the energy (2) with  $P = 0$  into eqs. (4) and (5). Eq. (4) yields the virial relation

$$\frac{J^2}{\mu r^2} = \frac{\mu M}{r}, \quad (6)$$

so that the equilibrium energy of a circular orbit becomes

$$E_{\text{eq}} = -\frac{1}{2} \frac{\mu M}{r}. \quad (7)$$

The orbital frequency of these orbits can be found from eq. (5) and satisfies, as expected, Kepler's third law

$$\Omega = \frac{\partial E}{\partial J} = \frac{J}{\mu r^2} = \sqrt{\frac{M}{r^3}}, \quad (8)$$

where we have used eq. (6) in the last equality.

Note that Newtonian point masses can be brought into arbitrarily close and arbitrarily tightly bound circular orbits. The orbits are stable for all separations  $r$ ,

indicating that in Newtonian point mass binaries there is no ISCO. As we will see, this is related to the gravitational interaction potential being proportional to  $1/r$ .

It is also illustrative to construct circular orbits graphically. In the left panel of Fig. 1, the solid lines are contours of the energy (2) at constant angular momentum. The minima of these contours correspond to circular orbits. Connecting these yields the equilibrium energy (7) as a function of separation.

## Tidal and relativistic effects

Compact binaries are extended, relativistic objects, of course, so that we have to take into account both tidal and relativistic effects.

For irrotational, identical stars, tidal effects can be modeled by adding a tidal interaction term

$$E_{\text{tidal}} = -2\lambda \frac{\mu M R^5}{r^6} \quad (9)$$

to the energy (2) (compare [5–7]), where  $R$  is the radius of the stars at large separations. The coefficient  $\lambda$  depends on how easily the stars can be deformed, and hence on their structure and equation of state (EOS). For polytropic EOSs with polytropic index  $n$  we have  $\lambda = (3/4) \kappa_n (1 - n/5)$ , where the coefficient  $\kappa_n$  is tabulated, for example, in [2]. For an incompressible fluid,  $\lambda = 3/4$ . Each star induces a quadrupole moment in the companion<sup>1</sup> which scales with  $1/r^3$ , and the two quadrupole moments' interaction again scales with  $1/r^3$ , so that  $E_{\text{tidal}} \sim r^{-6}$ .

From eq. (4), we can now find the equilibrium energy

$$E_{\text{eq}} = -\frac{1}{2} \frac{\mu M}{r} + 4\lambda \frac{\mu M R^5}{r^6}. \quad (10)$$

We immediately see that we can no longer construct arbitrarily tightly bound orbits, and that instead  $E_{\text{eq}}$  now assumes a minimum for a finite separation  $r$ . It is easy to show that any attractive interaction potential proportional to  $1/r^n$ ,  $n > 2$ , leads to a positive contribution to  $E_{\text{eq}}$ , and hence the existence of a minimum at finite  $r$ .

In the right panel of Fig. 1 we provide a graphical representation for incompressible fluid stars with  $m/R = 0.2$ , where  $m$  is the mass of the individual stars. For large separations, the tidal interaction is very small, and the orbits are similar to those of point masses. For small separations, however, the tidal interaction becomes dominant, and decreases the energy of a configuration with a given separation and angular momentum below that of the point mass binary. For large enough angular momentum, the  $J = \text{const}$  contours now have a maximum at a small separation in addition to the minimum at a larger separation, while for small angular momenta their contours no longer have any extrema. As a consequence, the equilibrium energy goes through a minimum. Outside of this minimum, the equilibrium energy

---

<sup>1</sup>) If the stars are not irrotational, the spin of the individual stars induces an intrinsic quadrupole moment. The tidal interaction energy then scales with a smaller power of  $r$ , see, e.g. [5,25]

curve connects minima of the  $J = \text{const}$  curves, which correspond to *stable* circular orbits, while inside this minimum, the curve connects maxima of  $J = \text{const}$  curves, which correspond to *unstable* circular orbits. The minimum of the equilibrium curve therefore marks the innermost stable circular orbit, the ISCO<sup>2</sup>.

We can similarly mimic relativistic effects by borrowing a relativistic interaction potential

$$E_{\text{rel}} = -\frac{M}{\mu} \frac{J^2}{r^3} \quad (11)$$

from the result for test particles in Schwarzschild space times. This interaction again gives rise to an ISCO. We mark the location of this ISCO in the left panel of Fig. 1, as well as the ISCO when computed from the combined tidal and relativistic effects. It is evident from this model calculation that including relativistic effects will move the ISCO to larger separation, and correspondingly smaller values of the orbital frequency  $\Omega$ .

Obviously, this model problem is very naive, and can at best mimic qualitative effects. However, it does illustrate several important results. Quite in general, the ISCO arises because of contributions to the interaction potential which deviate from a simple  $1/r$  scaling. In particular, tidal effects can cause an ISCO even in purely Newtonian systems. In general, both tidal and relativistic effects have to be taken into account for an accurate determination of the ISCO. Lastly, the model problem provides a straight-forward recipe for locating the ISCO: first construct circular orbits and the corresponding equilibrium energy  $E_{\text{eq}}$  by locating extrema of the energy (eq. (4)), then identify the ISCO with the minimum of  $E_{\text{eq}}$ , and last compute the orbital frequency  $\Omega$  from eq. (5). We have therefore reduced the problem of accurately determining the ISCO in black hole or neutron star binaries to an accurate determination of their energies, which we will address separately in the following sections.

## THE ISCO IN BINARY BLACK HOLES

Determining the ISCO in binary black hole systems has been attempted with two independent approaches: post-Newtonian expansions and numerical calculations in

---

<sup>2)</sup> At this point, a word of warning is in order. Relativistic binaries emit gravitational radiation, causing them to slowly spiral towards each other, and they hence do not follow strictly circular orbits. The very concept of an innermost stable *circular* orbit is therefore somewhat ill defined. Also, the minimum in the equilibrium energy identifies the onset of a *secular* instability, while the onset of *dynamical* instability may be more relevant for the binary inspiral (see, e.g., the discussion in [2] and also [3], where it is shown that the two instabilities coincide in irrotational binaries). Moreover, it has been suggested that the passage through the ISCO may proceed quite gradually [8], so that a precise definition of the ISCO may be less meaningful than the above turning method suggests. Ultimately, dynamical evolution calculations will have to simulate the approach to the ISCO and to investigate these issues. For the sake of dealing with a well-defined problem, we will here identify the ISCO with the minimum of the equilibrium energy.

full general relativity. We will outline both approaches, and will then compare the results.

## Post-Newtonian Calculations

A large number of researchers has developed post-Newtonian techniques to model compact objects in close binaries (an incomplete list includes [9–13]; see [14] for a particularly pedagogical treatment). Typically, these calculations start by bringing Einstein’s equations into the form

$$\square h^{\alpha\beta} = -16\pi\tau^{\alpha\beta} \equiv -16\pi(-g)T^{\alpha\beta} - \Lambda^{\alpha\beta}. \quad (12)$$

Here,  $\square$  is the flat space wave operator,  $h^{\alpha\beta}$  measures deviations from the flat Minkowski metric,  $g$  is the determinant of the metric, and the source term  $\tau^{\alpha\beta}$  contains both the stress-energy tensor  $T^{\alpha\beta}$  as well as non-linear terms in  $h^{\alpha\beta}$ , which have been absorbed in  $\Lambda^{\alpha\beta}$ . A formal solution to this equations is the retarded, flat-space Green function

$$h^{\alpha\beta}(t, \mathbf{x}) = 4 \int \frac{\tau^{\alpha\beta}(t', \mathbf{x}')\delta(t' - t + |\mathbf{x} - \mathbf{x}'|)}{|\mathbf{x} - \mathbf{x}'|} d^4x'. \quad (13)$$

Unfortunately, the source term  $\tau^{\alpha\beta}$  depends on the solution  $h^{\alpha\beta}$ , so that this formal solution is of little practical help. However, it can be used to construct a solution iteratively. Starting with a Newtonian point-mass solution, for which  $T_{\text{Newt}}^{\alpha\beta}$  is known and for which  $h^{\alpha\beta}$  vanishes, we can construct a first iteration from

$$\square h_1^{\alpha\beta} = 16\pi T_{\text{Newt}}^{\alpha\beta}. \quad (14)$$

Each solution  $h_n^{\alpha\beta}$  can be inserted on the right hand side of eq. (13), which then provides the next iteration  $h_{n+1}^{\alpha\beta}$ . Each iteration provides a correction over the previous one in the order of  $\epsilon \sim v^2 \sim m/R$ . The iteration therefore yields a post-Newtonian expansion of the solution  $h^{\alpha\beta}$ , from which the energy can be constructed in the form of a Taylor expansion

$$E_{\text{eq}} = E_{\text{Newt}} + E_1 \epsilon + E_2 \epsilon^2 + \dots \quad (15)$$

Here  $E_n \epsilon^n$  is the  $n$ -th order post-Newtonian correction to the energy.

It turns out, however, that for values close to the ISCO,  $\epsilon \sim 1/6$ , this expansion converges extremely slowly. The reason is that at a location fairly close to the ISCO, namely at the light radius with  $\epsilon \sim 1/3$ , some of the functions involved in the expansion diverge and have a pole (see [10]). It is therefore to be expected that a polynomial expansion of the form (15) will converge only very poorly in the neighborhood of that pole. Damour, Iyer and Sathyaprakash [10] provided a solution to this problem by using a resummation technique. Instead of employing the polynomial (15), they use the information contained in the Taylor expansion

to construct an expansion in terms of rational functions. To illustrate this with an example, assume that we know the Taylor expansion of an arbitrary function  $f(x)$  up to second order. We can then construct an expansion in terms of a rational function

$$f(x) \sim t_0 + t_1 x + t_2 x^2 + \dots \sim \frac{p_0 + p_1 x + \dots}{1 + q_1 x + \dots} \quad (16)$$

by choosing the coefficients  $p_0$ ,  $p_1$  and  $q_1$  such that the value and the first two derivatives of the two expansions match at  $x = 0$ . This expansion is known as a ‘‘Padé-approximant’’, and has been shown to greatly improve the convergence of post-Newtonian expansions at least up to second order.

When  $h_n^{\alpha\beta}$  is inserted on the right hand side of eq. (13), the integrals no longer have compact support, so that there is no guarantee that they will converge. Moreover, the use of point-mass sources gives rise to divergent integrals, which have to be re-normalized appropriately. This has been achieved up to second post-Newtonian order, but at third post-Newtonian order some ambiguities remain [11]. Damour, Jaranowski and Schäfer [13] have recently shown that these ambiguities can be expressed by a single dimensionless parameter,  $\omega_{\text{static}}$ , which is currently unknown. They compare three different post-Newtonian approaches (the  $e$ -method and  $j$ -method based on minimizations of the energy and the angular momentum, and an effective one-body method [12]) and find a quite remarkable result. For one particular choice of  $\omega_{\text{static}}$ , these three independent approaches yield very similar predictions for the angular momentum, energy, and orbital frequency at the ISCO. This self-consistency suggests that the correct values of  $\omega_{\text{static}}$  and the ISCO at 3PN order may have been identified.

## Numerical Calculations in General Relativity

A framework for numerically constructing models of binary black holes has been provided by Arnowitt, Deser and Misner’s 3+1 (ADM) decomposition of Einstein’s equations [15] and York’s conformal decomposition [16].

The ADM formalism splits Einstein’s equations into constraint and evolution equations. The gravitational fields, described by the spatial metric  $\gamma_{ij}$  and the extrinsic curvature  $K_{ij}$ , have to satisfy the constraint equations on each time slice, while the evolution equations describe how they evolve from one time-slice to the next. For the construction of initial data, the two constraint equations, the Hamiltonian constraint and the momentum constraint, have to be solved, which determine only the longitudinal parts of the gravitational fields. The transverse parts of the fields, loosely associated with the gravitational wave degrees of freedom, are unconstrained by the constraint equations, and have to be chosen before the constraints can be solved.

Since the binary inspiral outside the ISCO proceeds very slowly, the gravitational wave content of these spacetimes must be very small. It therefore seems reasonable

to attempt to minimize the gravitational wave content by choosing the spatial metric conformally flat,  $\gamma_{ij} = \psi^4 f_{ij}$ , where  $\psi$  the conformal factor and  $f_{ij}$  a flat metric. With the further assumption of maximal slicing,  $K \equiv \gamma^{ij} K_{ij} = 0$ , the Hamiltonian constraint reduces to

$$\hat{\nabla}^2 \psi = -\frac{1}{8} \psi^{-7} \hat{A}_{ij} \hat{A}^{ij}, \quad (17)$$

while the momentum constraint becomes

$$\hat{\nabla}_i \hat{A}^{ij} = 0. \quad (18)$$

Here  $\hat{\nabla}$  is the flat space covariant derivative, and  $\hat{A}^{ij}$  is the trace-free part of the conformally related extrinsic curvature,  $\hat{A}_{ij} = \psi^2 (K_{ij} - \gamma_{ij} K/3)$ . Quite remarkably, the momentum constraint (18) is now a linear equation and decouples from the Hamiltonian constraint. Solutions describing a pair of black holes with arbitrary momenta and spins can now be constructed analytically by super-imposing two solutions for single black holes [17]. Given these solutions, the Hamiltonian constraint (17) can then be solved numerically [18,19], which completes the construction of binary black hole initial data.

To construct binary black hole models in circular orbits and to determine their ISCO, turning points of the energy of these solutions have to be located, in complete analogy to the model problem above [20,21]<sup>3</sup>. These results have recently been generalized to binaries in which the individual black holes carry spin [22].

## Comparison

In Fig. 2, we summarize results from the post-Newtonian and numerical calculations. It is obvious that both the 2PN and 3PN results differ quite significantly from the numerical results, by more than a factor of two in the frequency. This discrepancy is very unsatisfactory, and should be resolved by re-examining both approaches and their assumptions.

The PN approach treats the binary stars as point-masses, and hence neglects tidal effects (even though these could be included, see, e.g., Appendix F of [14]). This approximation is probably fairly poor for binary neutron stars, but may be more adequate for binary black holes. Moreover, including tidal effects would probably move the ISCO to a larger separation and smaller orbital frequency, and would hence increase the discrepancy between the PN and numerical results. However, the convergence properties of the PN expansion and the lacking renormalization of higher-order expansion coefficients remain worrisome.

---

<sup>3</sup> The two approaches of [20] and [21] differ in the topology chosen for the binary black hole: [20] adopts the two-sheeted topology of [18], whereas [21] assumes the three-sheeted topology of [19]. Their results agree to within a few percent, indicating that this choice has little effect on the ISCO.



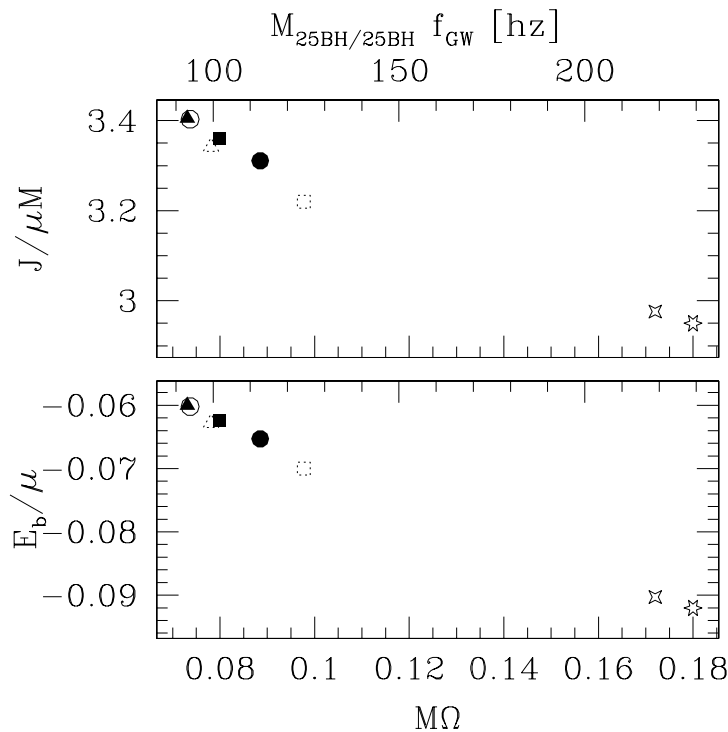


**FIGURE 2.** Results for the angular momentum, energy and orbital frequency of a black hole binary at the ISCO from post-Newtonian and numerical calculations. The solid triangle, square and circle are the 2PN results of [13] using the effective one-body method, the  $e$ -method, and the  $j$ -method. The open circle is their 3PN result, with the unknown parameter  $\omega_{\text{static}}$  chosen such that all three methods agree. The four-pointed and six-pointed star are the numerical results of [20] and [21]. The dashed triangle and square are 2PN results using the effective one-body and  $e$ -method together with a conformal-flatness assumption. The top label gives the corresponding gravitational wave frequencies for a binary of two  $25 M_{\odot}$  black holes.

The biggest worry in the numerical calculations is probably the assumption of conformal flatness. The effect of this assumption is evaluated in Appendix B of Ref. [13], where the authors determine the ISCO at 2PN order, using their effective one-body and  $e$ -method together with a conformal-flatness assumption. These results are included as the dashed triangle and square in Fig. 2. Obviously, this assumption changes the results somewhat, but not nearly enough to explain the discrepancy between the PN and numerical results. When evaluated for the effective one-body method, it even seems like conformal flatness is quite an adequate approximation.

None of the above more obvious worries seem to be able to completely explain the differences between the PN and numerical results. This suggests that perhaps the two approaches construct sequences which are not physically identical. In our discussion of the model problem above, we have implicitly assumed that the masses

$m_1$  and  $m_2$  of the binary stars remain constant during the inspiral. In general relativity, however, there is no unique definition of the mass of the individual black holes in a binary, and it is not clear which mass is conserved during the inspiral. It has been conjectured [23] that during the adiabatic inspiral outside of the ISCO the “irreducible mass” [24] of the black hole event horizons is conserved. In the numerical calculations of [18,21], this is approximated by the irreducible mass of the black hole apparent horizons<sup>4</sup>. In the PN approaches the masses  $m_1$  and  $m_2$  of the point sources are kept constant. It is not obvious that the two approximations are equivalent, and it is therefore possible that the two approaches construct physically distinct sequences.

## THE ISCO IN BINARY NEUTRON STARS

The ISCO in binary neutron stars has been computed in numerous Newtonian [2,5,25–27], PN [3,7,28] and relativistic calculations [29–31]. We will briefly summarize some of the qualitative findings of these calculations, and will then discuss some of the more recent relativistic results.

### Qualitative discussion

For binary neutron stars, the location of the ISCO depends on the physical properties of the individual stars, in particular their EOS and spin. Qualitatively, these effects can be illustrated by re-examining the tidal correction to the energy (9). Computing  $E_{\text{eq}}$  from (4) and (9), and then locating the minimum of  $E_{\text{eq}}$ , shows that the ISCO occurs at a separation

$$\frac{r_{\text{ISCO}}}{R} = (48\lambda)^{1/5} \quad (19)$$

and a frequency

$$m\Omega_{\text{ISCO}} = \sqrt{\frac{5}{2}} (48\lambda)^{-3/10} \left(\frac{m}{R}\right)^{3/2}. \quad (20)$$

Note that  $r_{\text{ISCO}}$  scales with the stellar radius  $R$ , and  $m\Omega_{\text{ISCO}}$  accordingly with  $(m/R)^{3/2}$ , where  $m/R$  is the stellar compaction (compare [25,7,31]).

The coefficient  $\lambda$  depends on the EOS. For polytropic EOSs,  $\lambda$  increases with decreasing polytropic index  $n$ . Eq. (19) therefore implies that  $r_{\text{ISCO}}/R$  is larger for stiffer EOSs. This explains why an ISCO exists only for stars with sufficiently stiff EOSs; for stars with too soft EOSs the stars merge before they encounter the ISCO. The critical value of  $n$  for the existence of an ISCO depends on the rotation

---

<sup>4</sup>) Locating an event horizon requires knowledge of a complete spacetime, while an apparent horizon can be located on a single timeslice.

of the stars and on relativistic effects, but is generally believed to be fairly close to  $n_{\text{crit}} \sim 1$ . Eq. (20) also implies that the ISCO frequency is correspondingly smaller for stiffer EOSs.

In the above discussion we have assumed that the stars are irrotational, so that  $E_{\text{tidal}} \sim r^{-6}$ . The effect of individual rotation can be estimated by allowing  $E_{\text{tidal}}$  to scale with a different power of  $r$  (compare [3,5,25]).

## Numerical Calculations in General Relativity

Constructing relativistic binary neutron stars requires solving the equations of relativistic hydrodynamics together with the initial value equations of general relativity. This problem can be simplified whenever the fluid flow is stationary, so that the equations of hydrodynamics reduce to a relativistic Bernoulli equation<sup>5</sup>.

This approach was first adopted by [29], who constructed corotational models of binary neutron stars in quasi-equilibrium. The initial value equations of general relativity were solved with the assumption that the spatial metric is conformally flat. For moderate (but realistic) compactions ( $m/R \lesssim 0.2$ ), for which the gravitational fields are only moderately strong, the latter assumption has been shown to be quite adequate (compare [32]). Results for various polytropic indices  $n$  and stellar compactions  $m/R$  can be found in [29]. For stars of  $1.4 M_{\odot}$ ,  $n = 1$  and  $m/R = 0.2$ , for example, they find a gravitational wave frequency at the ISCO of  $\Omega_{\text{ISCO}}^{\text{GW}} = 2 \Omega_{\text{ISCO}} \sim 1300$  Hz.

The viscosity in neutron star interiors is not believed to be strong enough to maintain corotation during binary inspiral [33]. It is therefore more realistic to assume the binary to be irrotational, in which case the relativistic equations of hydrodynamics can again be reduced to a Bernoulli equation [34]. Constructing irrotational binaries is computationally more complicated than constructing corotational binaries, because one of the boundary conditions has to be imposed on the surface of the stars. The location of the latter changes during the numerical iteration, and is a priori unknown. Nevertheless, several groups have succeeded in constructing relativistic, irrotational models of binary neutron stars [30].

Probably the most careful analysis to date of evolutionary sequences of irrotational binary neutron stars is presented in [31]. As pointed out earlier [30], the authors find that for moderately soft EOSs ( $n \gtrsim 2/3$ ), a cusp forms at the surface of the stars before an ISCO is encountered, at which point the numerical method breaks down. Most likely, the cusp indicates that a Lagrange point forms, and that matter starts to overflow towards the companion. The assumption of a stationary, irrotational fluid flow seems no longer adequate, and will have to be relaxed for the construction of closer binaries. An ISCO appears in these simulations only for fairly stiff EOSs ( $n \lesssim 2/3$ ). For these cases, the authors of [31] quite carefully

---

<sup>5</sup>) Note that a solution to the Bernoulli equation is by construction in equilibrium, and yields the equilibrium energy  $E_{\text{eq}}$ . For binary black holes the latter has to be constructed by finding turning points of the energy  $E$ .

analyze the ISCO for various compactness  $m/R$ , and show that it is dominated by the hydrodynamical effects of the tidal interaction. Up to moderate compactness ( $m/R \lesssim 0.2$ ), the relativistic effects can be expressed as PN corrections to the Newtonian scaling (20).

## SUMMARY

Knowledge of the ISCO may be an important ingredient for the future detection of gravitational wave signals and their interpretation. In this article we illustrate in a simple model problem how turning-point methods can be used to locate the ISCO (see, however, the disclaimer in footnote (2)). We also summarize recent efforts to determine the ISCO in both black hole and neutron star binary systems.

Currently, the biggest challenge for an accurate determination of the ISCO in binary black hole systems seems to be the disagreement between PN and numerical approaches. For binary neutron stars, we seem to be lacking a realistic description of the velocity field in close binaries. Ultimately, the quasi-equilibrium approaches presented in this paper should be backed up with fully dynamical simulations (e.g. [35]).

As a final comment, we point out that in this article we have only discussed binaries containing either black holes or neutron stars. So far black hole-neutron star binaries have only been modeled in Newtonian or PN dynamical simulations [36] and in ellipsoidal model calculations [37]. Such mixed binaries have yet to be constructed in a relativistic framework, and their ISCO (or the onset of tidal disruption) has yet to be determined self-consistently.

It is a pleasure to thank Greg Cook, Stuart Shapiro, and Masaru Shibata for numerous very useful discussions. The author gratefully acknowledges support through a Fortner Fellowship. This work was also supported by NSF Grant PHY 99-02833 at Illinois.

## REFERENCES

1. See contribution by B. C. Barish in this volume.
2. D. Lai, F. A. Rasio and S. L. Shapiro, *Astrophys. J. Suppl.* **88**, 205 (1993).
3. F. C. Lombardi, F. A. Rasio and S. L. Shapiro, *Phys. Rev. D* **56**, 3416 (1997).
4. T. W. Baumgarte, G. B. Cook, M. A. Scheel, S. L. Shapiro and S. A. Teukolsky, *Phys. Rev. D* **57**, 6181 (1998).
5. D. Lai, F. A. Rasio and S. L. Shapiro, *Astrophys. J.* **406**, L63 (1993).
6. D. Lai, *Phys. Rev. Lett.* **76**, 4878 (1996).
7. D. Lai and A. G. Wiseman, *Phys. Rev. D* **54**, 3958 (1996).
8. A. Buananno and T. Damour, *Phys. Rev. D* **62**, 084036 (2000); A. Ori and K. S. Thorne, submitted (2000), also gr-qc/0003032.

9. R. V. Wagoner and C. M. Will, *Astrophys. J.* **210**, 764 (1976); E. Poisson, *Phys. Rev. D* **47**, 1497 (1993); L. Blanchet, T. Damour, B.R. Iyer, C.M. Will and A.G. Wiseman, *Phys. Rev. Lett* **74** 3515 (1995);
10. T. Damour, B. R. Iyer and B. S Sathyaprakash, *Phys. Rev. D* **57**, 885 (1998).
11. P. Jaranowski and G. Schäfer, *Phys. Rev. D* **57**, 7274 (1998).
12. A. Buananno and T. Damour, *Phys. Rev. D* **59**, 084006 (1999).
13. T. Damour, P. Jaranowski and G. Schäfer, *Phys. Rev. D* **62**, 084011 (2000).
14. C. M. Will and A. G. Wiseman, *Phys. Rev. D* **54**, 4813 (1996).
15. R. Arnowitt, S. Deser and C. W. Misner, in *Gravitation: An Introduction to Current Research*, edited by L. Witten (Wiley, New York, 1962).
16. J. W. York, Jr., *Phys. Rev. Lett.* **26**, 1656 (1971).
17. J. Bowen and J. W. York, Jr., *Phys. Rev. D* **21**, 2047 (1980).
18. G. B. Cook, *Phys. Rev. D* **44**, 2983 (1991).
19. S. Brandt and B. Brügmann, *Phys. Rev. Lett.* **78**, 3606 (1997).
20. G. B. Cook, *Phys. Rev. D* **50**, 5025 (1994).
21. T. W. Baumgarte, *Phys. Rev. D* **62**, 024018 (2000).
22. H. P. Pfeiffer, S. A. Teukolsky and G. B. Cook, *Phys. Rev. D* **62**, 104018 (2000).
23. J. D. Bekenstein, in *Black Holes, Gravitational Radiation and the Universe*, edited by B. R. Iyer and B. Bhawal (Kluwer, Dordrecht, 1999).
24. C. Christodoulou, *Phys. Rev. Lett.* **25**, 1596 (1970).
25. D. Lai, F. A. Rasio and S. L. Shapiro, *Astrophys. J.* **420**, 811 (1994).
26. F. A. Rasio and S. L. Shapiro, *Astrophys. J.* **401**, 226 (1992); *Astrophys. J.* **432**, 242 (1994); *Astrophys. J.* **438**, 887 (1995); *Class. Quantum Grav.* **16**, R1 (1999).
27. K. C. B. New and J. E. Tohline, *Astrophys. J.* **490**, , (3)11 (1997).
28. M. Shibata, K. Taniguchi and T. Nakamura, *Prog. Theor. Phys. Suppl.* **128**, 295 (1997); M. Shibata, K.-I. Oohara and T. Nakamura, *Prog. Theor. Phys.* **98**, 1081 (1997).
29. T. W. Baumgarte, G. B. Cook, M. A. Scheel, S. L. Shapiro and S. A. Teukolsky, *Phys. Rev. Lett.* **79**, 1182 (1997); *Phys. Rev. D* **57**, 7292 (1998).
30. S. Bonazzola, E. Gourgoulhon and J.A. Marck, *Phys. Rev. Lett.* **82**, 892 (1999); P. Marronetti, G. J. Mathews and J. R. Wilson, *Phys. Rev. D* **60**, 087301 (1999); K. Uryu and Y. Eriguchi, *Phys. Rev. D* **61**, 124023 (2000); E. Gourgoulhon, P. Grandclement, K. Taniguchi, J.-A. Marck and S. Bonazzola, submitted (also gr-qc/0007028).
31. K. Uryu, M. Shibata and Y. Eriguchi, *Phys. Rev. D* **62**, 104015 (2000).
32. F. Usui, K. Uryu and Y. Eriguchi, *Phys. Rev. D* **61**, 024039 (2000).
33. L. Bildsten and C. Cutler, *Astrophys. J.* **400**, 175 (1992); C. S. Kochanek, *Astrophys. J.* **398**, 234 (1992).
34. S. Bonazzola, E. Gourgoulhon and J.-A. Marck, *Phys. Rev. D* **56**, 7740 (1997); H. Asada, *Phys. Rev. D* **57**, 7292 (1998); S. A. Teukolsky, *Astrophys. J.* **504**, 442 (1998); M. Shibata, *Phys. Rev. D* **58**, 024012 (1998).
35. M. Shibata and K. Uryu, *Phys. Rev. D* **61**, 064001 (2000).
36. See contributions by M. Ruffert and W. Lee in this volume.
37. M. Shibata, *Prog. Theor. Phys.* **96**, 917 (1996); P. Wiggins and D. Lai, *Astrophys. J.* **532**, 530 (2000); M. Vallisneri, *Phys. Rev. Lett.* **84**, 3519 (2000).